

## Supplementary information

### **Catalytically proficient ceria nanodots supported on redox-active mesoporous hosts for treatment of inflammatory bowel disease by efficient ROS scavenging**

Hailing Wang,<sup>#a</sup> Liucan Wang,<sup>#b</sup> Yuhua Chen,<sup>a</sup> Jixi Huang,<sup>a</sup> Yuxin Xing,<sup>a</sup> Lu Wang,<sup>a</sup> Jixi Zhang,<sup>\*,a</sup> and Hua Yang<sup>\*,b</sup>

<sup>a</sup> Key Laboratory of Biorheological Science and Technology, Ministry of Education, College of Bioengineering, Chongqing University, No. 174 Shazheng Road, Chongqing 400044, China

<sup>b</sup> Department of General Surgery, Chongqing People's Hospital, No.118, Xingguang Avenue, Liangjiang New Area, Chongqing 401121, China

\* Corresponding author.

E-mail address: jixizhang@cqu.edu.cn (Jixi Zhang); hwbyang@126.com (Hua Yang).

## **Supplementary Experimental data**

### **1. Characterization**

Transmission electron microscope (TEM) images were taken with a JEM 2010 (JEOL, Japan) instrument at an acceleration voltage of 200 kV for the characterization of morphology. The N<sub>2</sub> sorption isotherms were measured on an ASAP2010 analyzer (Micromeritics, USA). The Brunauer-Emmett-Teller (BET) method was employed to calculate the specific surface areas. The pore size distributions were derived from desorption branches of the isotherms by the NLDFT method. The hydrodynamic size distributions were acquired using dynamic light scattering (DLS) techniques on a Zetasizer Nano instrument (Malvern, UK) at 25°C. Raman spectra were obtained by using a dispersive spectrophotometer Jobin-Yvon LabRam HR Evolution with 532 nm light for sample excitation and a CCD detector cooled to -70°C. The laser power used was between 0.5 and 4 mW. Fourier transform infrared (FTIR) spectra were recorded on a Nexus 670 (Thermo Nicolet, USA) spectrometer.

### **2. Synthesis of MPDA NPs**

MPDA NPs were synthesized according to the previous report. First, 1.0 g F127 and 0.5 g DA were dissolved in 100 mL of a 1:1 mixture of water and ethanol and stirred vigorously at room temperature to obtain a clear solution. Then 2.0 mL of TMB was slowly injected into the solution with stirring speed of 500 rpm to form the nanoemulsion system. After stirring for 30 min, 5.0 mL of concentrated ammonia (NH<sub>4</sub>OH) was added dropwise to the above mixture to induce self-polymerization of dopamine oligomers. After 30 min of continuous reaction, the resulting dendritic mesoporous TMB/F127/PDA polymer nanospheres were centrifuged and washed at least three times with water and ethanol in turn. The mixed system was stirred at room temperature for 3 h and the precipitate was collected by centrifugation. The template was removed using extraction, i.e., the collected precipitate was dispersed with a mixture of ethanol and acetone (2:1, v/v) and sonicated for 30 min, centrifuged (11000 rpm, 15 min) and the supernatant discarded, and the sample was stored in ethanol after three repetitions.

### **3. Determination of Ce<sup>3+</sup> content**

The redox electrochemical properties of MPDA and MPDA@CeO<sub>2-x</sub> NPs were investigated by differential pulse voltammetry (DPV) using an electrochemical workstation (CHI700E, China). In the three-electrode electrochemical cell, glassy carbon was used as the working electrode, platinum wire as the counter electrode, and Ag/AgCl as the reference electrode.

X-ray photoelectron spectroscopy, i.e. compositional analysis, was performed on the nanomaterials using an ESCALAB-MKII spectrometer (Thermo Scientific K-Alpha, China). Before testing, aqueous solutions of MPDA, CeO<sub>2</sub> and MPDA@CeO<sub>2-x</sub> NPs were centrifuged and dried, and then a suitable dose of solid powder was taken for testing.

#### **4. Cell Culture**

Raw 264.7 macrophages were purchased from Shanghai Bogu Biotechnology Co., Ltd (China) and cultured in high sugar medium containing 10% (v:v) fetal bovine serum and 1% double antibiotics (penicillin: 100 U mL<sup>-1</sup>, streptomycin: 100 U mL<sup>-1</sup>) in a cell incubator at 37°C with 5% CO<sub>2</sub>. The cells were incubated at 37°C in a 5% CO<sub>2</sub> incubator, and fresh cell culture medium was changed every two days.

#### **5. *In vitro* antioxidant and anti-inflammatory mechanism of MPDA@CeO<sub>2-x</sub> NPs by regulating the Nrf2/NF-κB pathway.**

Immunofluorescence staining and Western blot were performed on different groups of Raw 264.7 macrophages to detect HIF-1α, Nrf2 and NF-κB proteins.

**Immunofluorescence staining:** Immunofluorescence staining was performed to detect the expression and localization of nuclear factor 2 (Nrf2). Raw 264.7 cells were inoculated into φ15 confocal dishes at a density of 1.5×10<sup>5</sup> per well and incubated overnight in a cell incubator. After pretreatment with different concentrations of MPDA@CeO<sub>2-x</sub> (20-60 μg mL<sup>-1</sup>) for 24 h, the cells were cultured in hypoxic medium containing LPS (1 μg mL<sup>-1</sup>) for 12 h. Macrophages without LPS stimulation were used as a control group. Macrophages were then washed with PBS, after which they were fixed in 4% paraformaldehyde for 10 min. Macrophages were then washed with PBS and incubated with an anti-p-Nrf2 antibody (1:1000 dilution, Abcam) for 12 h at 4°C. After PBS washing, samples were incubated with FITC-labeled goat anti-rabbit IgG

antibody (1:1000 dilution, Abcam) and nuclei were stained with DAPI, and finally images were acquired by laser scanning confocal microscopy.

Western blot (WB) analysis: inflammation model was induced using lipopolysaccharide (LPS) stimulation of Raw 264.7 cells, and cellular proteins were separated by 10% sodium dodecyl sulfate polyacrylamide gel electrophoresis (SDS-PAGE) and transferred to polyvinylidene fluoride (PVDF) membranes. After being closed in 5% bovine serum albumin (BSA) for 2 h, the membranes were incubated with HIF-1 $\alpha$  (1:1000), p-Nrf2 (1:1000), NF-KB p65 (1:1000) and  $\beta$ -Actin (1:1000) primary antibodies, respectively, overnight at 4°C. After washing with TBS containing 0.05% Tween 20 (TBST), the membrane was incubated with horseradish peroxidase (HRP)-coupled secondary antibody (1:500) for 1 h at 37°C, followed by membrane imaging. The  $\beta$ -actin, HIF-1 $\alpha$ , p-Nrf2 and NF- $\kappa$ B p65 protein expression were quantified separately using ImageJ software.

Mouse colonic mucosal proteins were separated by 10% sodium dodecyl sulfate polyacrylamide gel electrophoresis (SDS-PAGE) and transferred to polyvinylidene fluoride (PVDF) membranes. After being closed in 5% bovine serum albumin (BSA) for 2 h, membranes were incubated overnight at 4°C with primary antibodies: Occludin (1:1000), Claudin-1 (1:1000) and  $\beta$ -Actin (1:1000). After washing with TBS containing 0.05% Tween 20 (TBST), the membranes were incubated with horseradish peroxidase (HRP)-coupled secondary antibody (1:500) for 1 h at 37°C, followed by membrane imaging.

## **6. CCK-8 Assay**

Raw 264.7 macrophages were first inoculated in 96-well plates ( $1 \times 10^4$  cells per well) for 24 h. After incubation, the original medium was removed and the cells were exposed to different concentrations of MPDA, CeO<sub>2</sub> and MPDA@CeO<sub>2-x</sub> suspensions (0, 10, 25, 50, 100 and 200  $\mu\text{g mL}^{-1}$  of fresh medium). After co-culture for 24 h, the original medium was removed and washed twice with PBS. Fresh culture medium (100  $\mu\text{L}$ ) containing 10% Cell Counting Kit (CCK-8) was added and incubated for 1 h protected from light. Finally, the absorbance of the culture medium in each well was measured at 450 nm using a Bio-Rad 680 ELISA, and the cell activity was calculated

by comparison with the control, which led to the cytotoxicity value.

### **7. *In vivo* fluorescence imaging**

The *in vivo* distribution of MPDA@CeO<sub>2-x</sub> was investigated by loading IR780 into MPDA@CeO<sub>2-x</sub>. After transrectal administration of IR780 (20 mg kg<sup>-1</sup>) and IR780-loaded MPDA@CeO<sub>2-x</sub> NPs, 2.5% DSS-induced mice were anesthetized with isoflurane gas at different time points after execution of DSS-induced mice and dissection of the colon. The fluorescence intensity of MPDA@CeO<sub>2-x</sub> NPs loaded with IR780 in the colon of each mouse was recorded using a small animal *in vivo* imager (IVIS).

### **8. Polymerase Chain Reaction (PCR)**

To further understand the therapeutic mechanism of MPDA@CeO<sub>2-x</sub> in IBD, the expression levels of major inflammatory factors (TNF- $\alpha$ , IL-1 $\beta$  and IL-6) in the colon tissue of mice in each group were detected by polymerase chain reaction. Total RNA was extracted from homogenized colonic tissues using TRIzol reagent. RNA quality was determined by measuring the optical density at the ratio of 260 nm and 280 nm and cDNA was synthesized by reverse transcription. The expression levels of major inflammatory factors in colon tissues after different treatments were detected by qRT-PCR.

### **9. Evaluation of Systemic Safety of MPDA@CeO<sub>2-x</sub> in Mice**

Blood samples were collected from mice in EP tubes, placed on ice, and 10  $\mu$ L was added to 90  $\mu$ L of diluent and mixed well for serum biochemical parameters and routine blood tests. The main organs (heart, liver, spleen, lung and kidney) of mice were taken for histological sectioning and stained by H&E for histopathological examination. In addition, the remaining blood was placed at 4°C for more than 2 h protected from light, centrifuged at 5000 rpm for 15 min, and the supernatant was collected to determine liver functions, mainly aspartate aminotransferase (AST) and alanine aminotransferase (ALT) in liver function for safety testing. The toxicity of the MPDA@CeO<sub>2-x</sub> group was studied at a high dose (20 mg kg<sup>-1</sup>) (10-fold higher than the therapeutic experiment (2 mg kg<sup>-1</sup>) described above).

Supplementary Figures

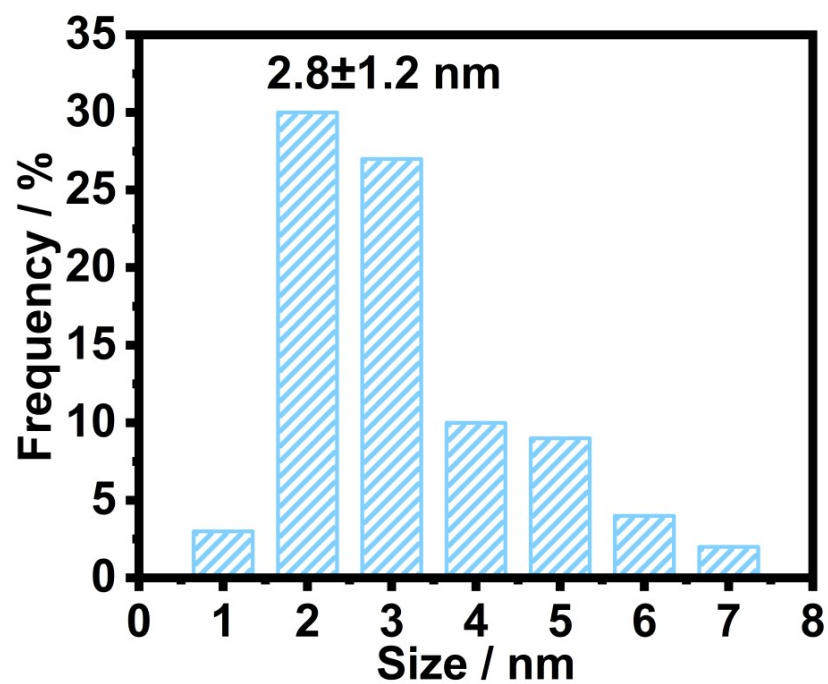
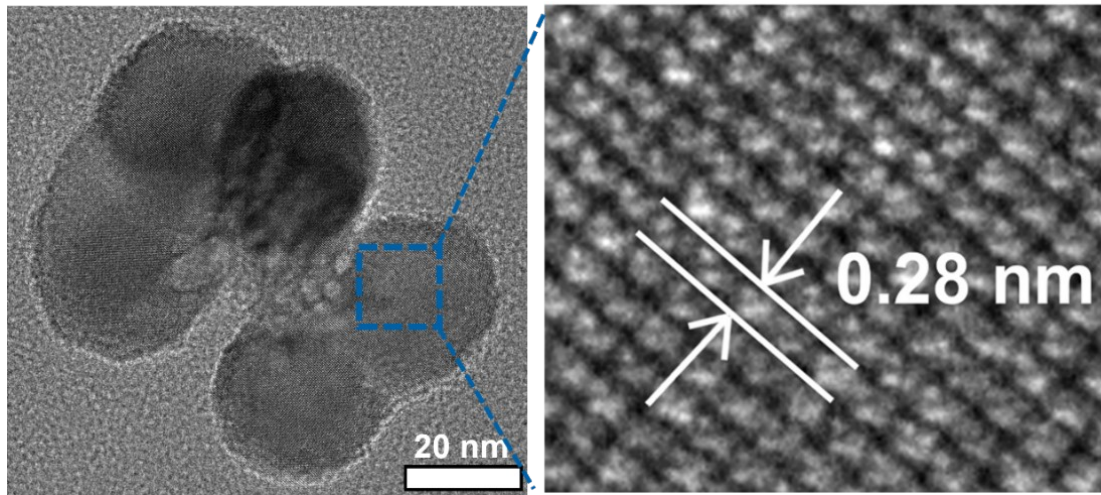
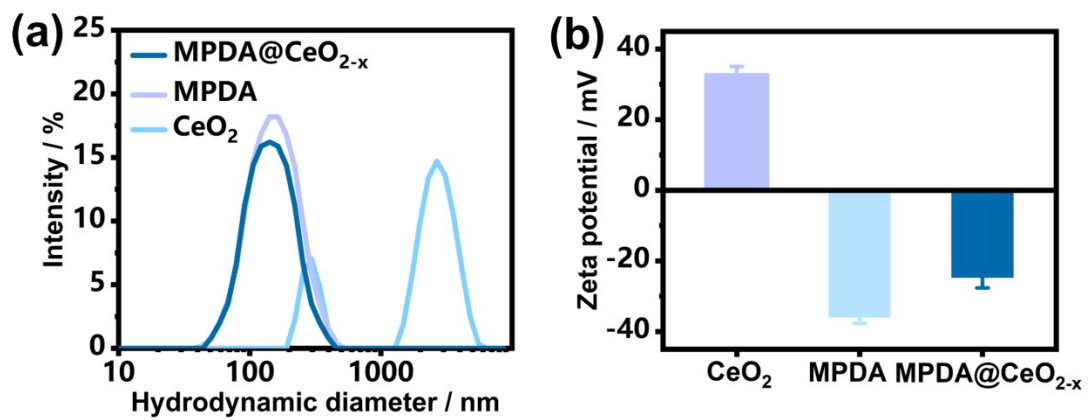


Figure S1. Size distribution of CeO<sub>2-x</sub> NPs on the surface of the hybrid nanosystems.



**Figure S2.** TEM and lattice images of CeO<sub>2</sub> nanoparticles.



**Figure S3.** (a) Dynamic light scattering results and (b) Zeta potential of different nanoparticles (mean  $\pm$  SD; n =5).

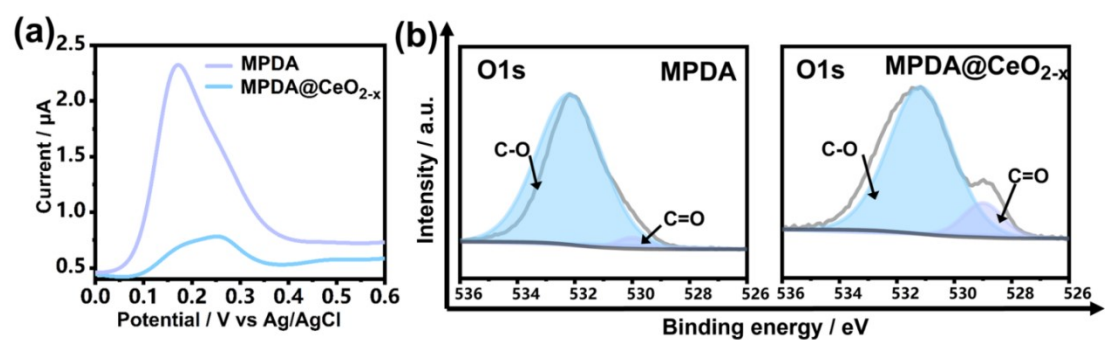


**Figure S4.** (a) DPV curves of MPDA and MPDA@CeO<sub>2-x</sub> nanoparticles; (b) O1s high-resolution XPS spectrum of MPDA and MPDA@CeO<sub>2-x</sub> nanoparticles.

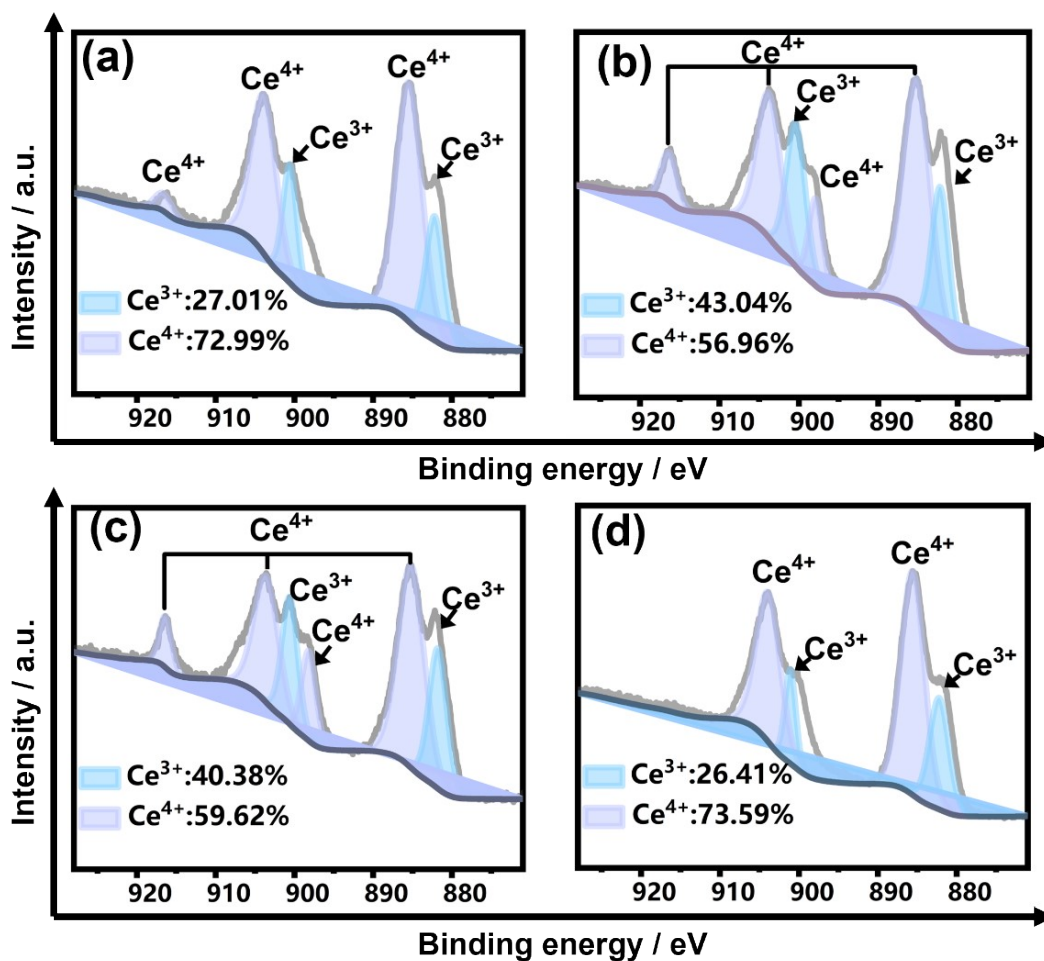


**Figure S5.** High-resolution map of the Ce 3d of MPDA@CeO<sub>2-x</sub> at different feed ratios: where the mass ratios of Ce(Ac)<sub>3</sub>·nH<sub>2</sub>O/MPDA are 0.4 (a), 1.0 (b), 1.50 (c) and 2.33 (d), respectively.

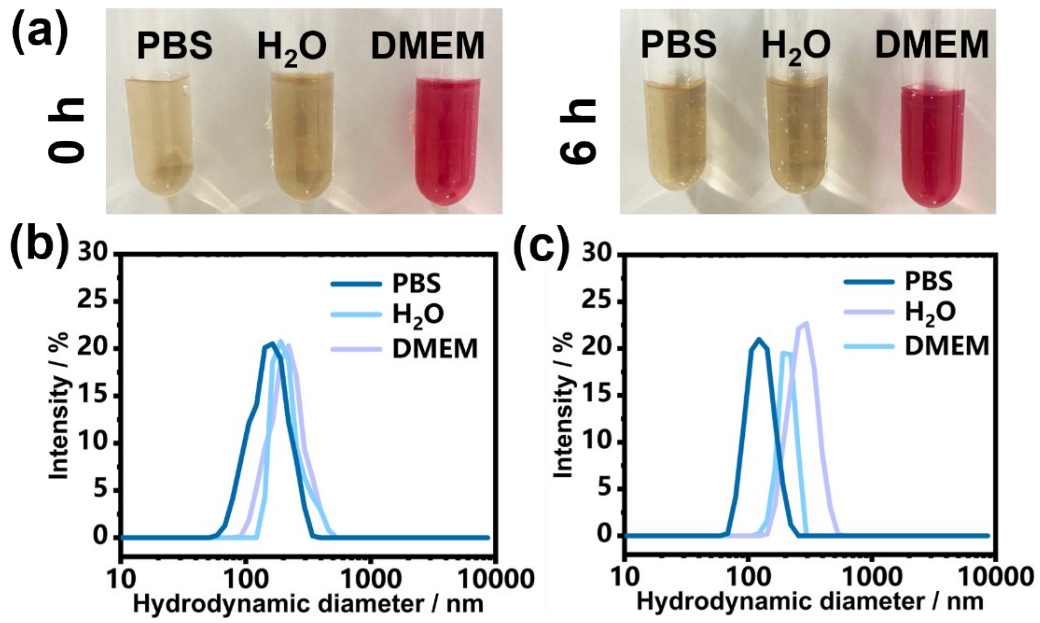


**Figure S6.** (a) MPDA@CeO<sub>2-x</sub> sample photos in different liquids (PBS buffer, water and culture medium) for different times (0/6 h), and (b, c) the corresponding hydrodynamic diameters.

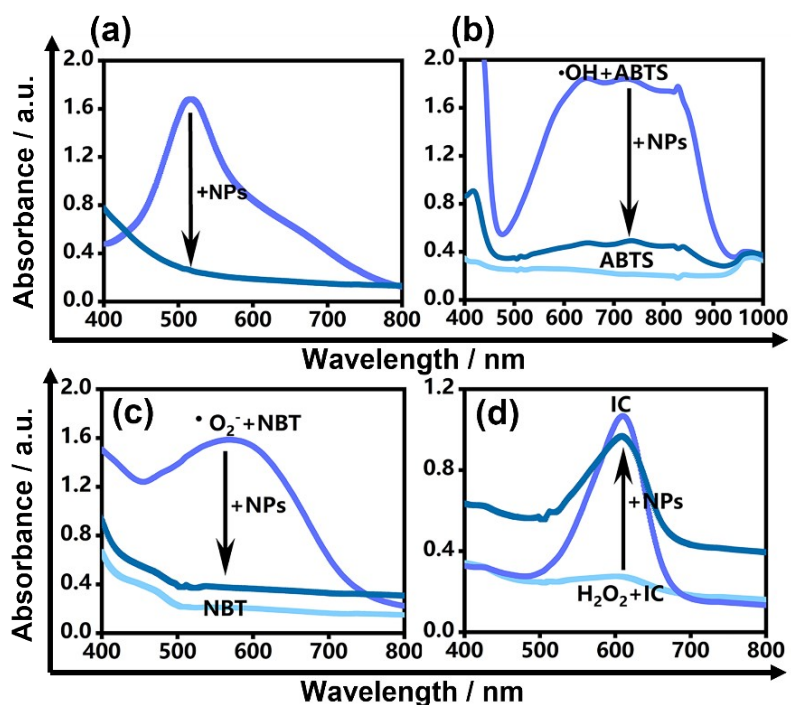


**Figure S7.** (a) Changes of the visible-near-infrared absorption spectrum of DPPH before and after treatment with MPDA@CeO<sub>2-x</sub> (100 μg mL<sup>-1</sup>); (b) changes of visible-near-infrared absorption spectra of ABTS in blank control and with/without MPDA@CeO<sub>2-x</sub> after Fe<sup>2+</sup> and H<sub>2</sub>O<sub>2</sub> treatment; (c) MPDA@CeO<sub>2-x</sub> (100 μg mL<sup>-1</sup>) changes of visible-near-infrared absorption spectra of NBT before and after treatment: blank control, no UV radiation, UV radiation, UV radiation in the presence of NPs; (d) visible-near-infrared absorption spectrum changes of indigo carmine (IC) dye solution after different treatments: blank control and with/without MPDA@CeO<sub>2-x</sub> condition.

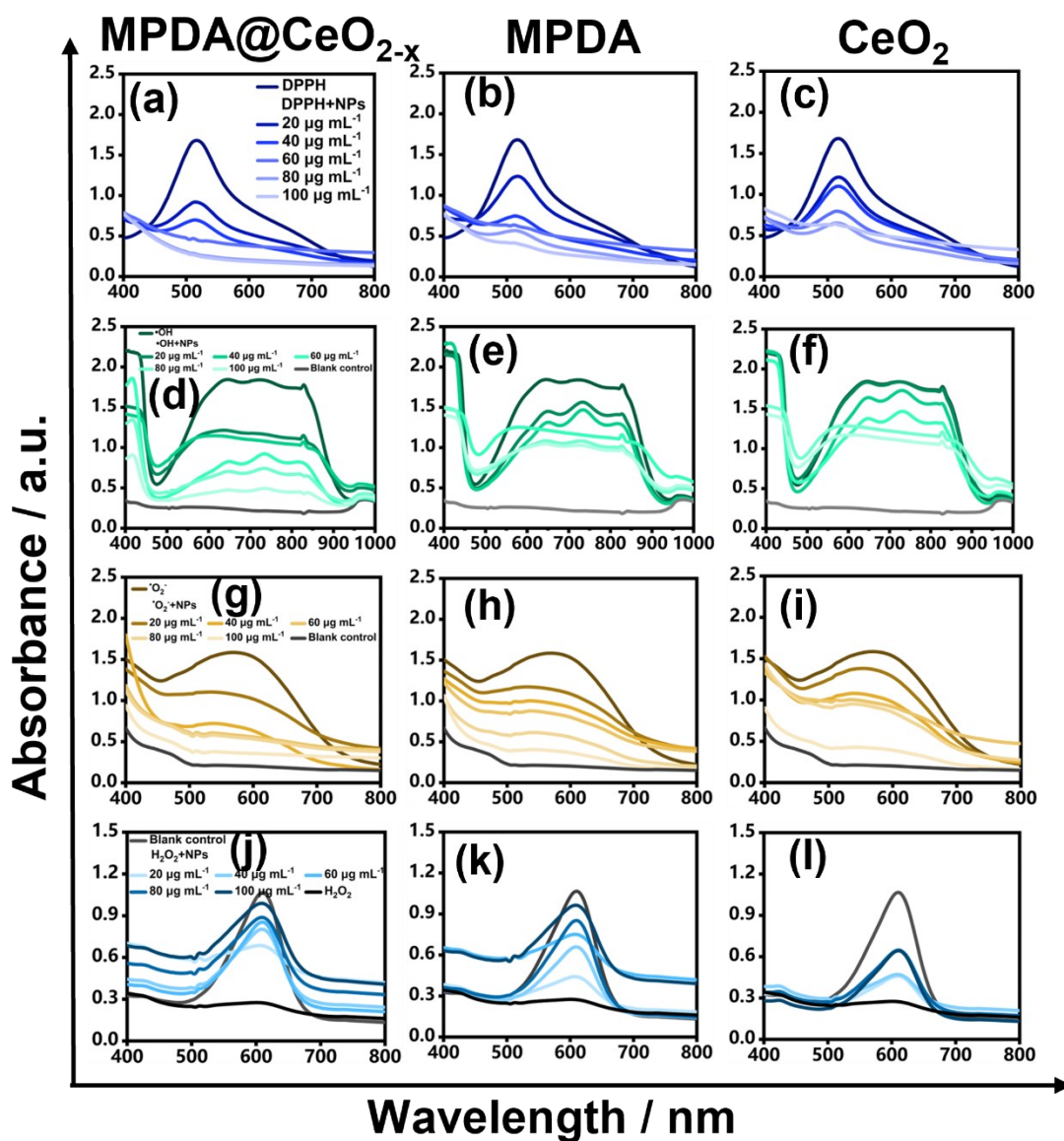


**Figure S8.** Vis-NIR absorption spectra of DPPH after treated with MPDA@CeO<sub>2-x</sub> (a), MPDA (b), and CeO<sub>2</sub> (c) at different concentrations (0-100 μg mL<sup>-1</sup>); absorption spectra of ABTS (d-f), NBT (g-i), and indigo carmine (j-l) after different treatments.

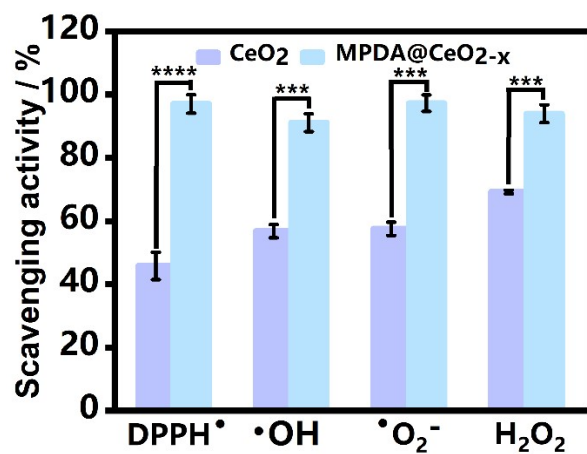


**Figure S9.** Scavenging efficiency of MPDA and MPDA@CeO<sub>2-x</sub> with the same cerium ion content toward different ROS.

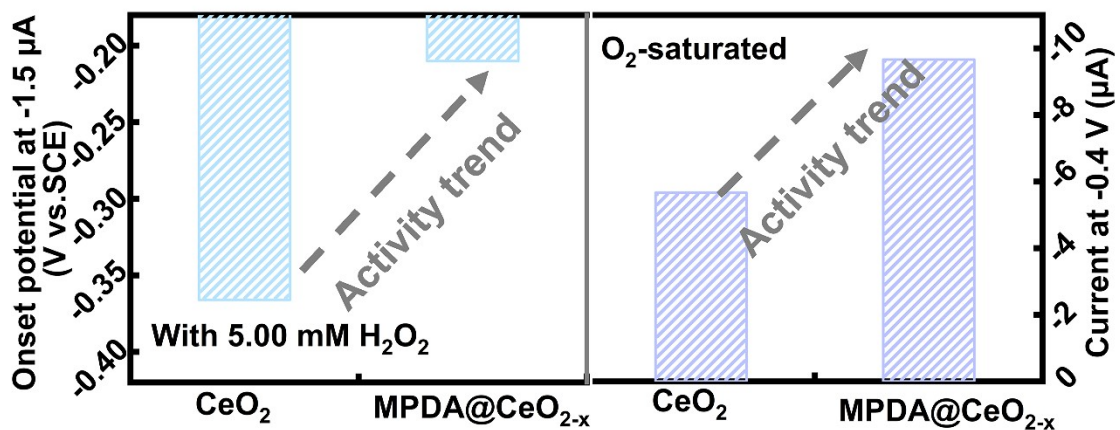
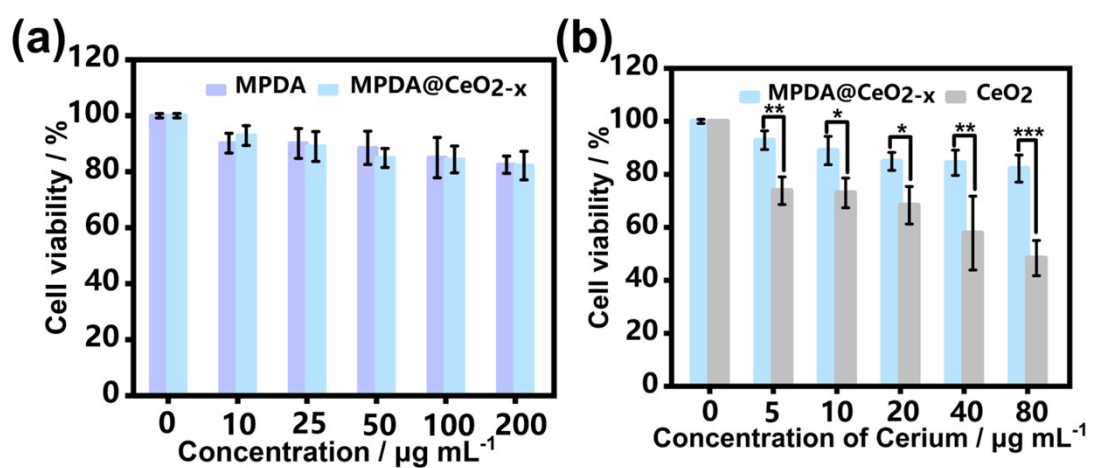
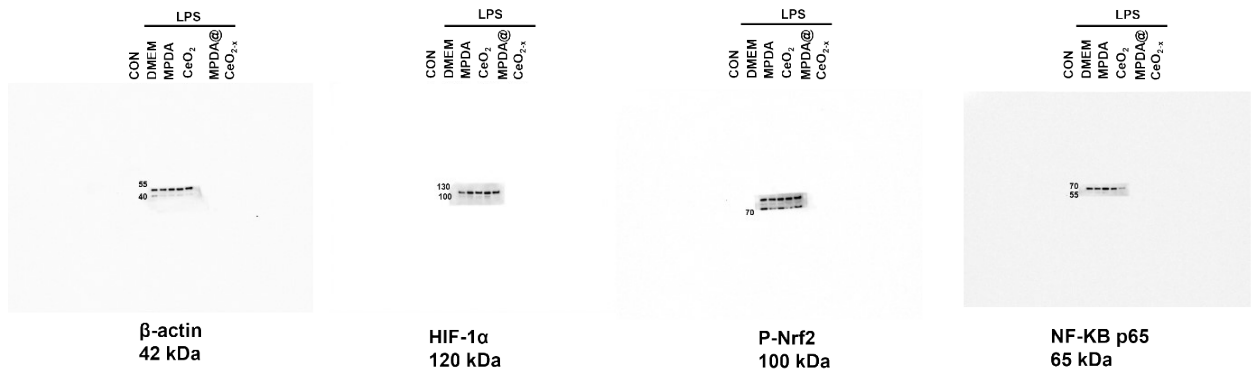


Figure S10. H<sub>2</sub>O<sub>2</sub> and oxygen reduction activities in terms of onset potential and current.



**Figure S11.** (a) Cell viability of Raw 264.7 macrophages treated with MPDA and MPDA@CeO<sub>2-x</sub> nanoparticles; (b) Viability of Raw 264.7 macrophages treated with MPDA@CeO<sub>2-x</sub> and CeO<sub>2</sub> nanoparticles containing the same content of cerium ions (mean ± SD; n =5) \*p<0.05, \*\*p<0.01, \*\*\*p<0.001.



**Figure S12.** Western blot analysis of HIF-1 $\alpha$ , p-Nrf2 and NF- $\kappa$ B P65 (NF- $\kappa$ B inflammatory pathway) in each group, with  $\beta$ -actin as control.

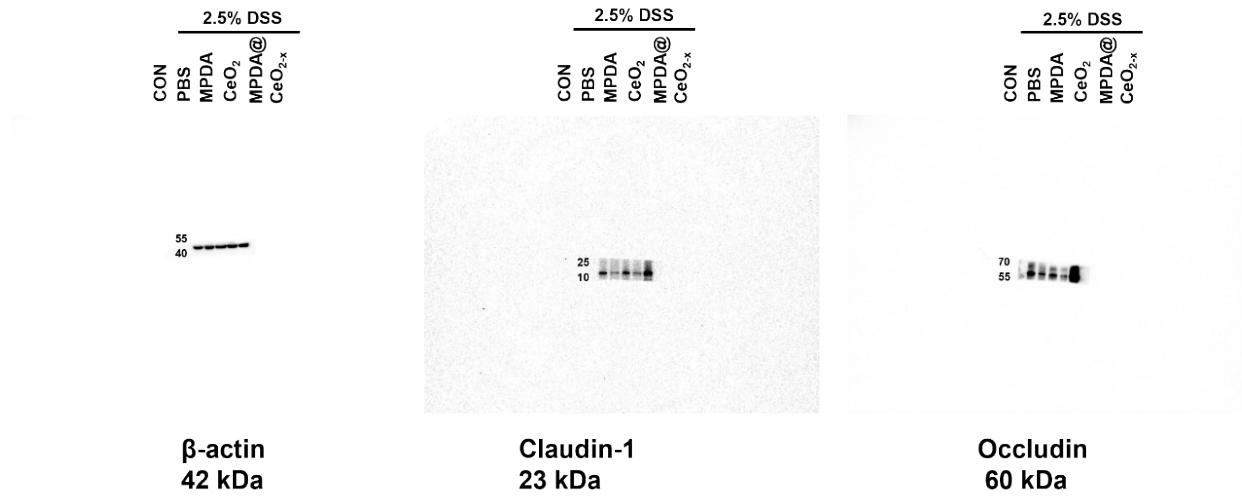


**Figure S13.** Western blot analysis of tight junction proteins expression in colonic mucosa.

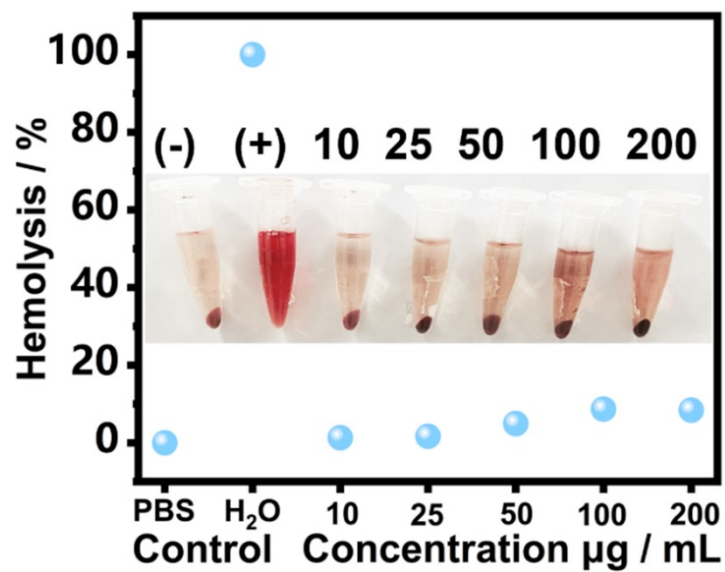


**Figure S14.** Hemolysis data of hemocytes incubated with varying concentrations (10-200  $\mu\text{g mL}^{-1}$ ) of MPDA@CeO<sub>2-x</sub> nanoparticles for 30 min. The inset shows a photo of the sample after incubation and centrifugation.

**Table S1 Disease activity Index scoring criteria for colitis**

Weight loss	Degree of rectal occult blood	Shape of feces	Score
No weight loss	Normal stool color	Normal	0
1%-5%	Brown dung	Soft stools or stools that form on the walls of the cage	1
5%-10%	Light red bloody stool	Unformed feces	2
10%-15%	Dark red blood stool	Watery stool	3
>15%		A liquid stool that moistens the hair around the anus	4

**Table S2 Colonic injury scoring criteria**

Degree of inflammation	Range of inflammation	Degree of crypt loss	Score
No	No	No	0
Mild	Intrinsic layer	Basal 1/3 damaged	1
Moderate	Mucosa and submucosa	Basal 2/3 damaged, surface epithelium intact	2
Severe	Translucent wall	Loss of the entire crypt and epithelium	3